

Accessible, At-Home Detection of Parkinson's Disease via Multi-task Video Analysis

MD SAIFUL ISLAM, TARIQ ADNAN, SANGWU LEE, ABDELRAHMAN ABDELKADER, and EHSAN HOQUE, Department of Computer Science, University of Rochester, USA

JAN FREYBERG, Google Research, Health AI, UK

CATHE SCHWARTZ and KAREN JAFFE, InMotion, USA

MEGHAN PAWLIK, Center for Health + Technology, University of Rochester Medical Center, USA

RUTH B. SCHNEIDER and E RAY DORSEY, Department of Neurology, University of Rochester Medical Center, USA

ABSTRACT

Background

Limited access to neurological care leads to missed diagnoses of Parkinson's disease (PD), leaving many individuals unidentified and untreated. While AI-driven video analysis has identified Parkinsonian symptoms from single motor or speech tasks, models trained on multiple tasks will be more robust.

Methods

We trained a novel neural network based fusion architecture to detect Parkinson's disease (PD) by analyzing features extracted from webcam recordings of three tasks: finger tapping, facial expression (smiling), and speech (uttering a sentence containing all letters of the alphabet). Additionally, the model incorporated Monte Carlo Dropout to improve prediction accuracy by considering uncertainties. The study participants were randomly split into three sets: 60% for training, 20% for model selection (hyper-parameter tuning), and 20% for final performance evaluation. An online demonstration of the tool is available at <https://parktest.net/demo>.

Results

The dataset consists of 1102 sessions from 845 participants (with PD: 272, female: 445, mean age: 61.9), each session containing videos of all three tasks. Our proposed model achieved significantly better accuracy, area under the ROC curve (AUROC), and sensitivity at non-inferior specificity compared to any single-task model. Withholding uncertain predictions further boosted the performance, achieving 88.0% (95% CI: 87.7% - 88.4%) accuracy, 93.0% (92.8% - 93.2%) AUROC, 79.3% (78.4% - 80.2%) sensitivity, and 92.6% (92.3% - 92.8%) specificity, at the expense of not being able to predict for 2.3% (2.0% - 2.6%) data. Further analysis suggests that the trained model does not exhibit any detectable bias across sex and ethnic subgroups and is most effective for individuals aged between 50 and 80.

Conclusions

A video analytics tool assessing finger tapping, facial expression, and voice demonstrates promising accuracy in differentiating individuals with PD from those without. This accessible, low-cost approach requiring only an internet-enabled device with webcam and microphone paves the way for convenient PD screening at home, particularly in regions with limited access to clinical specialists.

Authors' addresses: Md Saiful Islam, mislam6@ur.rochester.edu; Tariq Adnan; Sangwu Lee; Abdelrahman Abdelkader; Ehsan Hoque, Department of Computer Science, University of Rochester, Rochester, New York, USA; Jan Freyberg, Google Research, Health AI, London, UK; Cathe Schwartz; Karen Jaffe, InMotion, Beachwood, Ohio, USA; Meghan Pawlik, Center for Health + Technology, University of Rochester Medical Center, Rochester, New York, USA; Ruth B. Schneider; E Ray Dorsey, Department of Neurology, University of Rochester Medical Center, Rochester, New York, USA.

INTRODUCTION

Limited access to neurological care, particularly in remote areas and low-income countries contributes to the underdiagnosis of Parkinson's disease (PD), the fastest-growing neurological disorder [7, 8]. A delay in diagnosis and treatment may significantly impact quality of life. Traditionally, a diagnosis of PD is made by a clinician on the basis of history and examination which may include completion of a set of standardized tasks and rating each task following the Movement Disorder Society Unified Parkinson's Disease Rating Scale (MDS-UPDRS) [9]. Recently, a cerebrospinal fluid based α -synuclein seed amplification assay has been developed [22], that may serve as a diagnostic biomarker. However, diagnostic methods relying on the collection of CSF are invasive, costly, and burdensome to the patient. Recent research has employed machine learning and sensors to assess PD remotely. Nocturnal breathing signals obtained from a breathing belt or reflected radio signal can detect PD with high accuracy when analyzed by a machine learning model [27], and several body worn sensors have been successfully used to monitor clinical features like dyskinesia and gait disturbances associated with PD [16]. However, there are still limitations to using wearable sensors including cost, comfort, and ease of use, which makes it difficult to scale these techniques for global use. Therefore, readily accessible alternatives to the existing diagnostic methods are crucial for enabling timely intervention and improved patient outcomes.

Video analysis presents a convenient solution. Imagine, anyone can visit a website on a computer, turn on the webcam and microphone, and complete a set of standardized tasks. Using the advances in computer vision and machine learning, precise clinical features can be extracted from the recorded videos, and used to screen for PD [12] or track symptom progression [11]. However, existing methods for video analysis suffer from two major limitations – small datasets [12], and single modality [2, 11, 20, 24] (see Supplementary Note 3, where we provide a comprehensive summary of existing approaches). Symptoms of PD are multi-faceted, and affect individuals differently. For instance, one individual may face speech difficulty while retaining relatively normal motor functionality, while another individual may have prominent hypomimia (i.e., reduced facial expression) or bradykinesia (i.e., in-coordination of movements). Therefore, PD detection models may need to consider all of these modalities for improved efficacy.

Here, we employed a multi-task video analysis approach using the largest available dataset of recorded videos. The dataset consists of webcam recordings of individuals completing three tasks – (i) finger-tapping (motor function), (ii) smile (facial expression), and (iii) pangram (i.e., sentence containing all the letters of the alphabet) utterance (speech). 845 unique participants recorded all of these tasks successfully (some of them multiple times), resulting in 1102 videos for each task, and a total of 3306 videos. Each of the tasks are first modeled with a separate neural network trained with Monte Carlo dropout (MC-dropout) to provide a task-specific prediction and uncertainty of the prediction. We propose a novel uncertainty-calibrated fusion network (neural-network based model), that combines features from multiple tasks using cross-attention to generate a final PD/non-PD prediction, while calibrating the attention scores based on task-specific uncertainty. The model is also trained with MC-dropout so that the confidence of the final prediction can be modeled and predictions with low confidence can be withdrawn for patient safety. Overall, the proposed video analysis enables accessible, precise, and remote detection of PD. An overview of our proposed tool is shown in Figure 1a.

METHODS

Data Collection

Standardized Tasks. We selected three standardized tasks that can be easily completed using a computer webcam and microphone, with or without external supervision:

- (i) **Finger-tapping:** participants tap their thumb finger with the index finger ten times, as fast as possible. Tapping is done with the right hand first, and then with the left hand. Finger-tapping task is completed in

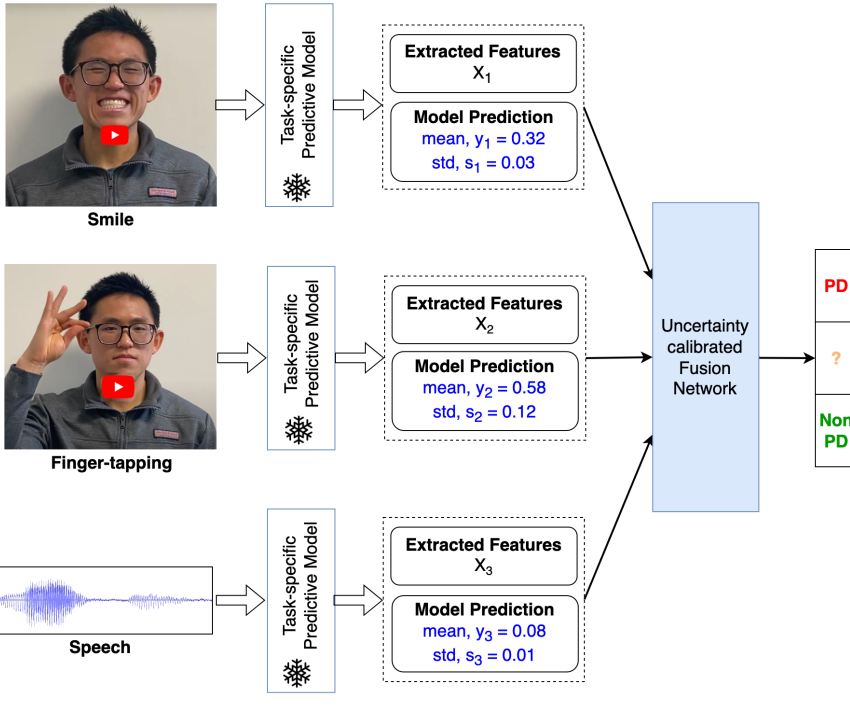
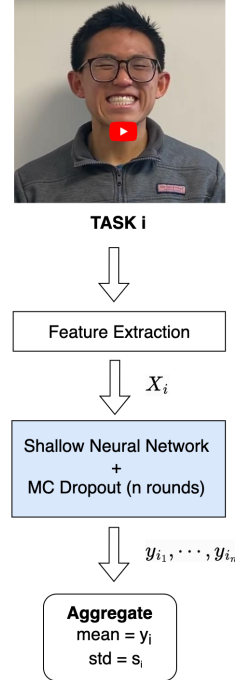
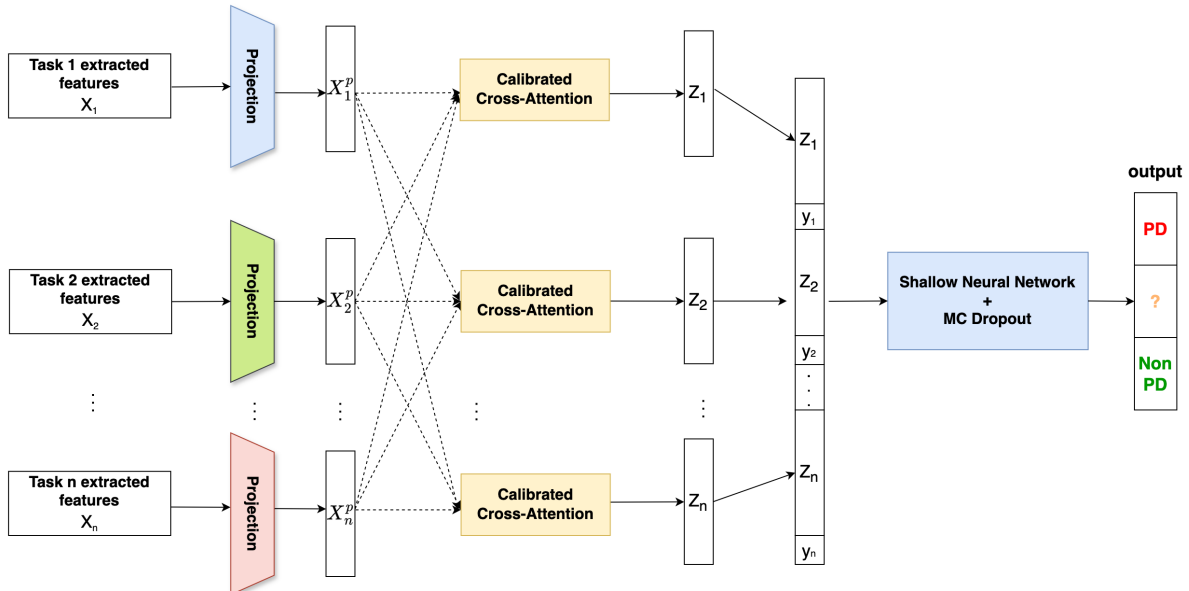
a. Overview**b. Task-specific Model****c. Uncertainty-calibrated Fusion Network, *UFNet***

Fig. 1. (a) An illustrative overview of the proposed PD detection tool, (b) Task-specific models that are trained independently with videos of a single task, and (c) architecture of the proposed UFNet model that combines features from three standardized tasks. Authors have obtained consent for publishing images of the human subject.

accordance with the MDS-UPDRS [9] scale to measure bradykinesia (i.e., slowness of movement) in the upper limb, a key sign of PD [10].

- (ii) **Smile:** participants mimic a smile expression three times slowly, alternating with a neutral face. Although the expression may not be natural, studies suggest it still captures signs of hypomimia (i.e., reduced expressiveness), which is a key indicator in PD diagnosis [2, 5].
- (iii) **Speech:** participants utter an English pangram, “*The quick brown fox jumps over a lazy dog. The dog wakes up, and follows the fox into the forest. But again, the quick brown fox jumps over the lazy dog.*” The first sentence contains all the letters of the English alphabet, and the later sentences are added to obtain a longer speech segment. Prior research identified this task as a promising way of screening PD [20].

Study Participants. We recruited participants through multiple methods – use of a brain health study registry, social media outreach, recruiting via InMotion (a wellness center for individuals with PD, located in Ohio, US), and clinician referrals. The study is approved by the University of Rochester Institutional Review Board. About 1,400 unique participants recorded at least one of the three standardized tasks, and 845 participants (272 with PD) recorded all three tasks. InMotion clients recorded the tasks using a laptop located at the care facility, and participants recruited from the clinical studies recorded the tasks from a clinic. Other participants completed the recordings primarily at their home. InMotion clients and clinician referred participants went through clinical diagnosis (using standardized criteria) to determine whether they had PD. The home-based participants self-reported their PD diagnosis. Table 1a summarizes the demographic information of the participants.

Dataset. Although the majority of the participants completed all three tasks, some did not complete one or more tasks. Some task videos were also discarded due to feature extraction failure, primarily due to participants’ failure to follow task instructions. Instead of completely discarding the videos of participants with missing tasks, we train task-specific models with all available videos for that task, potentially strengthening the modeling of each individual task. The multi-task model is then trained on the participants who completed all three tasks. We split the datasets based on the participants to ensure patient-centric evaluation. First we listed all the participants ($n = 1402$) enrolled in the study, and then randomly assigned 60%, 20%, and 20% of the participants into the training, validation, and test sets respectively. Therefore, both task-specific and multi-task models are validated and tested on the same participant cohort, and none of the models see any data from these participants during training. A detailed overview of the dataset splits is provided in Table 1b.

Feature Extraction

We rely on prior literature to extract clinically meaningful features for each task. Although state-of-the-art deep learning models eliminate the need for feature extraction as they learn to represent a video during training [15, 23], these models would require a significantly larger dataset to be trained effectively. Once a task-video is converted into a set of features, the problem can be modeled with simpler models having significantly less number of trainable parameters. Here, we briefly describe the task-specific features and refer to prior literature for details.

- (i) **Finger-tapping features:** Islam et al. [11] extracted 65 features to analyze the finger-tapping task for assessing PD severity. The feature extraction employs MediaPipe hand to detect the movements of a specific hand (i.e., left or right) and obtain the hand key-points. Using the key-points, clinically meaningful features such as finger-tapping speed, amplitude, interruptions, can be objectively measured. We employ their technique to extract the features for both hands by running the extractor twice (first for the left hand, and again for the right hand). Therefore, we extract 130 features in total for the finger-tapping task.
- (ii) **Smile features:** We leveraged the same 42 facial features extracted by Adnan et al. [2] from smile mimicry videos. These features, captured using OpenFace and MediaPipe, encompass key Parkinson’s disease markers outlined by the MDS-UPDRS, such as eye blinking, lip separation, mouth opening, and intensity of

Table 1. (a) Demographic information of the participants who completed all three tasks. With PD column represents the participants with Parkinson's disease, Without PD column represents the participants who do not have Parkinson's disease. (b) The dataset contains videos of three different tasks: finger-tapping (motor function), smile (facial expression), and speech (pangram utterance) from 1167, 1357, and 1265 participants, respectively. For some participants, one or more task videos are missing. Notably, 845 unique participants (including 272 with Parkinson's disease) have videos for all three tasks. Validation and test set participants are the same across the tasks (participants with missing videos are excluded).

(a) Demographic information				
Subgroup	Attribute	With PD	Without PD	Total
	Number of participants	272	573	845
Sex, n(%)	Female	122 (44.9%)	323 (56.4 %)	445 (52.7%)
	Male	147 (54.0%)	250 (43.6 %)	397 (47.0%)
	Nonbinary	1 (0.4%)	0 (0.0 %)	1 (0.1%)
	Unknown	2 (0.7%)	0 (0.0 %)	2 (0.2%)
Age in years, n (%) (range: 18.0 - 93.0, mean: 61.9)	Below 20	0 (0.0 %)	6 (1.0 %)	6 (0.7 %)
	20-29	1 (0.4 %)	28 (4.9 %)	29 (3.4 %)
	30-39	2 (0.7 %)	19 (3.3 %)	21 (2.5 %)
	40-49	6 (2.2 %)	17 (3.0 %)	23 (2.7 %)
	50-59	33 (12.1 %)	119 (20.8 %)	152 (18.0 %)
	60-69	94 (34.6 %)	231 (40.3 %)	325 (38.5 %)
	70-79	98 (36.0 %)	76 (13.3 %)	174 (20.6 %)
	80 and above	12 (4.4 %)	4 (0.7 %)	16 (1.9 %)
	Unknown	26 (9.6 %)	73 (12.7 %)	99 (11.7 %)
Ethnicity, n (%)	American Indian or Alaska Native	1 (0.4 %)	0 (0.0 %)	1 (0.1%)
	Asian	3 (1.1 %)	34 (5.9 %)	37 (4.4%)
	Black or African American	3 (1.1 %)	29 (5.1 %)	32 (3.8%)
	white	163 (59.9 %)	463 (80.8 %)	626 (74.1%)
	Others	2 (0.7 %)	3 (0.5 %)	5 (0.6%)
	Unknown	100 (36.8 %)	44 (7.7 %)	144 (17.0%)
Recording environment, n (%)	Home	39 (14.3 %)	399 (69.6 %)	438 (51.8 %)
	Clinic	91 (33.5 %)	107 (18.7 %)	198 (23.4 %)
	PD wellness center	142 (52.2 %)	67 (11.7 %)	209 (24.7 %)

Task/Split	Dataset size	Unique	With PD
	Number of videos, PD %	participants	n (%)
Finger-tapping	1374, 41.3%	1167	427 (36.6%)
Training	945, 43.9%	819	318 (38.8%)
Validation	221, 37.6%	172	56 (32.6%)
Test	208, 33.2%	176	53 (30.1%)
Smile	1684, 32.8%	1357	387 (28.5%)
Training	1021, 33.2%	824	234 (28.4%)
Validation	342, 33.9%	266	76 (28.6%)
Test	321, 30.5%	267	77 (28.8%)
Speech	1655, 33.9%	1265	366 (28.9%)
Training	1007, 35.3%	769	223 (29.0%)
Validation	338, 33.7%	252	73 (29.0%)
Test	310, 29.7%	244	70 (28.7%)
All tasks	1102(×3), 41.8%	845	272 (32.2%)
Training	690, 45.1%	516	168 (32.6%)
Validation	215, 38.1%	167	55 (32.9%)
Test	197, 34.9%	162	49 (30.2%)

facial muscle movements. Notably, machine learning models trained solely on this feature set demonstrated promising performance [2].

(iii) **Speech features:** We extracted 1024-dimensional embeddings from a pre-trained WavLM [6] language model to encode the pangram utterance task. WavLM excels at understanding audio due to its training on massive amounts of speech data. This training allows WavLM to capture the acoustic characteristics of speech, making it useful for various tasks like speech recognition, speaker identification, and even emotion recognition in voices. Recent research has also shown WavLM embeddings to be effective for PD screening [1].

Model Training

Task-specific Models. Each task utilizes a separate machine learning model to distinguish between individuals with and without PD. These models have three main components:

- **Optional feature selection and scaling:** Pairwise correlation among the features are calculated based on the training data. If two features have a Pearson’s correlation coefficient (PCC) above a specified threshold, then one feature is dropped. Finally, feature values were optionally scaled using `StandardScaler` or `MinMaxScaler` algorithms. Whether to apply feature selection or scaling, correlation threshold, and scaling method are hyper-parameters tuned on the validation set.
- **Shallow neural networks:** The shallow neural network consists of one or two linear layers (0-1 hidden layer), the last layer consisting a single output neuron. The hidden layer is followed by a non-linear `ReLU` activation function, while the output layer is followed by a `sigmoid` function.
- **Monte Carlo (MC) dropout:** To improve model robustness and estimate prediction uncertainty, we employ MC dropout [4]. This technique involves training the model with dropout (a method to prevent overfitting) and then performing multiple prediction rounds during testing. This allows us to capture the variability in predictions and estimate confidence in the final result.

After running the model with MC dropout for n rounds, we obtain n different predictions for the same data. These predictions allow us to estimate two key values:

1. Predicted Probability of PD (y): This is the average of the n predictions, representing the model’s confidence that the input indicates Parkinson’s disease.
2. Uncertainty in the Prediction (s): The standard deviation of the n predictions reflects the model’s certainty in its prediction. A higher standard deviation indicates greater uncertainty.

We categorize the results based on a threshold (i.e., 0.5). If the average prediction is above this threshold, the model suggests a positive test for PD, otherwise negative. The model is trained using a binary cross-entropy loss, along with an optimizer (like SGD or AdamW) and a learning rate – hyper-parameters fine-tuned on the validation set. Figure 1b illustrates the essence of the task-specific models. Please refer to Supplementary Note 1 where we provide the hyper-parameter choices for each task-specific model.

Uncertainty-calibrated Fusion Network, UFNet. The fully trained task-specific models remain frozen during the training of *UFNet*. For each task i , the extracted features (X_i with dimension d_{X_i}), predicted PD probability (y_i), and uncertainty in the prediction (s_i) are input to the *UFNet*. The model then combines information from all the tasks through a series of steps to generate a final, more robust prediction of PD probability (Figure 1c):

Projection: Since the size of the features may vary from task to task, they are first projected to same dimension (d) using a projection layer. Each of the projection layers consists of a linear layer ($\mathbb{R}^{d_{X_i}} \rightarrow \mathbb{R}^d$) with MC dropout, followed by non-linear activation (`ReLU`) and layer normalization.

Calibrated cross-attention: Cross-attention is a specific type of attention [26] mechanism used in models that deal with multiple inputs. It allows the model to focus on relevant parts of one input sequence when processing

another. The projected task-specific features (X_i^P) are converted to queries (q_i), keys (k_i), and values (v_i) via multiplying them by the associated matrices (W^Q, W^K, W^V , respectively) that are learned during training. Attention weights are calculated based on the similarity between the queries and keys. For example, when processing the projected task-specific features X_i^P , we obtain the query as $q_i = W^Q \cdot X_i^P$ from the same task, and the keys $k_j = W^K \cdot X_j^P$ are computed from all tasks. The dot product of q_i and k_j , known as the attention score, determines how much attention should be given to the features of task j when processing task i . Here, we calibrate the attention scores to penalize the tasks with highly uncertain task-specific predictions. Specifically, if the attention scores of the three tasks are a_1, a_2 , and a_3 and the task-specific uncertainties are s_1, s_2 , and s_3 , then the attention scores are re-calculated with $(a'_1, a'_2, a'_3) = \text{softmax}(a_1 - \eta s_1, a_2 - \eta s_2, a_3 - \eta s_3)$, where η is a hyper-parameter. The `softmax` function ensures that the sum of the attention scores is 1. After computing the attention scores, X_i^P is converted into contextualized representation $Z_i = \sum_{j=1}^{j=N} (a'_j \cdot v_j)$, where $N = 3$ is the number of tasks.

Shallow neural network: The contextualized representations (Z_1, Z_2, Z_3) obtained after cross-attention are concatenated along with the task-specific predicted probabilities (y_1, y_2, y_3), and the merged vector is now input to a shallow neural network similar to the one used for task-specific training. The network is trained with 30 rounds of MC dropout, and the average output of these 30 rounds is used as the final prediction (PD if the average output is more than 0.50, non-PD otherwise).

Withholding predictions: Since we obtain multiple predictions based on different rounds of random dropout, we can model the confidence of the predictions. We compute the 95% confidence interval of the predicted scores, and if the interval contains the decision threshold (i.e., 0.50), the prediction is considered to be of low confidence. For patient safety, we withhold such predictions, as these are more likely to be inaccurate.

The model is trained with binary cross entropy loss and SGD optimizer with momentum 0.6898. After hyper-parameter tuning on the validation set, the query dimension is set to 64 with 0.0207 learning rate, 0.4960 dropout probability, and $\eta = 81.8179$. Supplementary Note 2 details the hyper-parameter search procedure.

Multimodal Baselines

We compare our proposed *UFNet* with four popular choices of combining multimodal data.

Majority Voting. The predictions from three different task-specific models are combined to generate a single prediction. The predicted class (PD, Non-PD) agreed by the majority (i.e., two or more) is the final prediction.

Neural Late Fusion. The logit scores (i.e., PD probability) obtained from the task-specific models are input to a shallow neural network that learns to combine these predictions into a single binary prediction. This approach is equivalent to logistic regression or other ensembling methods.

Early Fusion Baseline. The features obtained from all three tasks are concatenated together and passed as an input to a shallow neural network, similar to the ones used in *UFNet* or the task-specific models. The final layer of the network is a single neuron that learns to classify between PD and Non-PD.

Hybrid Fusion Baseline. In addition to the task-specific features, task-specific prediction scores (logits) are also provided as input to a shallow neural network. The network can focus on both the input features and the prediction scores, enabling it to reap the benefits of both early and late fusions.

By default, the input to the *UFNet* is the task-specific features and prediction scores, making it a hybrid fusion approach. In addition, we analyze the effect of removing the task-specific predictions from the *UFNet*, as an early fusion approach. We also analyze the effect of withholding predictions for both early and hybrid versions of *UFNet*.

Model Selection and Performance Reporting

Highest AUROC on the validation set predictions was used to select the best performing model (i.e., hyper-parameters) for the reported experiments. The hyper-parameter search is detailed in Supplementary Notes 1 and 2. After hyper-parameter selection, each model is run with 30 different random seeds and the best hyper-parameters, and evaluated on the test set. For each performance metric, the average of 30 runs and the 95% confidence interval is reported.

Since the dataset is imbalanced, we report accuracy, balanced accuracy (average of sensitivity and specificity), F_1 score, AUROC, and AUPRC (area under the precision-recall curve) to compare the holistic performance of the models. We also report specificity, sensitivity, positive predictive value (PPV), and negative predictive value (NPV) of the *UFNet* model and other multi-task baselines. Coverage (% of cases where a prediction is given) is reported when uncertain predictions are withheld. Unless otherwise specified, significant difference means no overlap in the 95% confidence intervals, while non-inferiority means overlap in the intervals.

In addition to reporting traditional performance metrics, we also evaluate the calibration of the final, selected model. A well calibrated model's prediction scores can approximate the true probability of positive class. For example, if an ideally calibrated model predicts a PD probability of 90% for 100 individuals, the model will be correct for 90 individuals, while being incorrect for 10 individuals. A well-calibrated model may enable safe use, as the model can communicate prediction confidence (i.e., the likelihood of a correct prediction). In order to evaluate calibration, we use two popular metrics: expected calibration error (ECE) [17], and Brier score [21].

Finally, we compared the miss-classification rates across male and female subgroups to analyze whether the proposed model demonstrates any bias based on participants' sex. For statistical significance testing, we used two-sampled Z -test for proportions. Also, we compared model performance across white and non-white participants in the test set. Due to having a small number of non-white participants in the test set, we used Fisher's exact test to investigate whether there was any significant bias based on ethnicity. We also report the average miss-classification rate and their corresponding confidence intervals of the model across different age groups. Note that, we did not run the model with 30 random seeds for these subgroup analyses. Rather, we used the hyper-parameters (including the seed) that performed the best (i.e., best AUROC) on the validation set.

RESULTS

The study collected data from 1402 unique participants, who recorded the videos from three different environments: home, clinic, and a wellness center. Although the participants were instructed to complete all the three tasks used in this study, some did not record one or more tasks, and in some cases, feature extraction failed due to quality issues. Participants with missing tasks (or failed feature extraction) were ignored for the analysis of multi-task model, resulting in 1102 usable data samples from 845 participants to train and evaluate the model (Table 1b). Among the 845 participants, 272 had PD (39 self-reported and 233 clinically diagnosed). While both females and males participated evenly, the majority were over 50 years of age (667, 78.9%) and white (626, 74.1%) (see Table 1a).

Speech is the most accurate task for PD detection

Among the three standardized tasks we have explored, pangram utterance (speech) seems to be the most accurate for classifying individuals with and without PD. Only taking speech features as input, shallow neural network achieved 84.48% (95% CI: 84.19% - 84.78%) accuracy and 89.37% (89.19% - 89.55%) AUROC. Finger-tapping has the least accuracy for PD detection. For this task, we explored model training on features extracted from left or right hand alone, or on both hands. Model trained only on the right-hand tapping features performs significantly better (in most metrics) than the left-hand based model. However, the model trained on concatenated features from both hands significantly improves the F_1 score while being non-inferior in other metrics. Therefore, for the remaining part of the manuscript, finger-tapping model would refer to the one trained on both-hands tapping features. For all

Table 2. (a) Comparison of performance among models trained on different single tasks, (b) Performance of task-specific models after applying Monte Carlo dropout, and (c) Performance of models trained on different combinations of the three standardized tasks. Underlined metrics denote significantly better performance compared to other configurations of the same task, while **bold** metrics denote the significant, best performance across all choices. The braces denote 95% confidence intervals. All the metrics should be interpreted as percentages (%).

(a) Task-specific models					
Task	Accuracy	Balanced Accuracy	F_1 score	AUROC	AUPRC
Finger-tapping					
Both hands	72.0 [71.1, 72.9]	69.0 [68.1, 70.0]	<u>60.2</u> [58.9, 61.5]	73.9 [73.1, 74.8]	58.9 [57.9, 59.8]
	64.3 [62.9, 65.6]	62.0 [60.7, 63.4]	52.6 [50.8, 54.5]	66.9 [65.3, 68.6]	51.8 [50.2, 53.4]
Left hand	73.0 [72.3, 73.7]	70.0 [68.9, 71.1]	47.3 [44.4, 50.2]	73.7 [72.5, 75.0]	58.5 [57.0, 60.0]
	75.6 [75.4, 75.8]	72.2 [72.0, 72.4]	64.3 [63.9, 64.6]	83.2 [83.0, 83.3]	64.9 [64.6, 65.1]
Smile					
Speech	84.5 [84.2, 84.8]	82.5 [82.0, 82.9]	71.7 [71.2, 72.1]	89.4 [89.2, 89.6]	81.9 [81.6, 82.3]
(b) Task-specific models with MC dropout					
Task	Accuracy	Balanced Accuracy	F_1 score	AUROC	AUPRC
Finger-tapping					
Without MC Dropout	72.0 [71.1, 72.9]	69.0 [68.1, 69.9]	60.2 [58.9, 61.5]	73.9 [73.1, 74.8]	58.9 [57.9, 59.8]
	73.1 [72.5, 73.8]	70.1 [69.4, 70.8]	61.7 [60.7, 62.6]	74.9 [74.2, 75.6]	58.1 [57.2, 59.0]
Smile					
Without MC Dropout	75.6 [75.4, 75.8]	72.2 [72.0, 72.4]	64.3 [63.9, 64.6]	83.2 [83.0, 83.3]	64.9 [64.6, 65.1]
	77.6 [77.4, 77.8]	74.4 [74.2, 74.6]	67.5 [67.2, 67.8]	83.6 [83.6, 83.7]	65.4 [65.2, 65.5]
Speech					
Without MC Dropout	84.5 [84.2, 84.8]	82.5 [82.0, 82.9]	71.7 [71.2, 72.1]	89.4 [89.2, 89.6]	81.9 [81.6, 82.3]
	85.1 [84.8, 85.3]	83.8 [83.3, 84.3]	72.1 [71.4, 72.7]	87.8 [87.6, 87.9]	80.7 [80.4, 81.0]
(c) Multi-task combinations					
Task Combination	Accuracy	Balanced Accuracy	F_1 score	AUROC	AUPRC
Finger-tapping + Smile + Speech					
	87.3 [86.9, 87.7]	86.4 [86.0, 86.8]	81.0 [80.4, 81.6]	92.8 [92.6, 93.0]	86.3 [85.8, 86.8]
Finger-tapping + Smile					
	78.0 [77.1, 78.8]	75.1 [74.1, 76.1]	65.6 [64.0, 67.3]	84.8 [83.3, 85.3]	74.5 [73.9, 75.2]
Finger-tapping + Speech					
	84.1 [83.8, 84.4]	82.4 [82.0, 82.7]	77.3 [76.9, 77.7]	91.4 [91.2, 91.6]	86.5 [86.2, 86.8]
Smile + Speech					
	85.2 [84.9, 85.5]	82.8 [82.4, 83.3]	75.0 [74.7, 75.4]	91.2 [91.0, 91.3]	82.2 [81.7, 82.7]

metrics reported, the model trained on smile features performs better than the finger-tapping task, but worse than the speech task. Please see Table 2a for detailed performance reporting.

The effect of applying MC dropout while training the task-specific neural networks is mixed (see Table 2b). MC dropout significantly boosts the performance of the smile model (in all metrics). On the other hand, although MC dropout significantly improves the accuracy and balanced accuracy of the speech model, the AUROC and AUPRC is significantly decreased. However, due to additional benefits of MC dropout in modeling prediction uncertainty, we train the multi-task models (*UFNet* and other baselines) with MC dropout unless specified otherwise.

Multi-task combinations perform better than single-task models

Combining multiple tasks together using the proposed *UFNet* model enhances the performance in general (Table 2c). For instance, the AUPRC score of the multi-task models are significantly better than their corresponding single-task scores. Although the finger-tapping task alone is the weakest for detecting PD, the features from this task act as complementary to other task features, resulting in significant improvement in most metrics. Most notably, combining all the three tasks together significantly improves all the reported metrics, resulting in an accuracy of 87.29% (86.93% - 87.66%), AUROC of 92.81% (92.60% - 93.01%), and F1 score of 80.96% (80.35% - 81.58%).

Table 3. Comparison of *UFNet* performance against multimodal baselines. The underlined metrics indicate significantly better performance compared to all four baselines. **Bold** metrics indicate overall best performance across all choices. All scores should be interpreted as percentages (%). Confidence interval is not reported for majority voting since it does not involve any randomness.

Model	Accuracy	Balanced Accuracy	AUROC	AUPRC	F ₁ score	PPV (Precision)	NPV	Sensitivity (Recall)	Specificity	Coverage
Majority Voting	85.28	83.94	89.59	77.98	78.20	80.0	87.88	76.47	89.92	-
Neural Late Fusion	84.08	81.32	91.73	86.66	73.17	73.47	89.16	76.32	88.17	-
	[81.68, 86.48]	[76.49, 86.14]	[89.50, 93.96]	[83.56, 89.76]	[64.85, 81.49]	[65.92, 81.01]	[86.11, 92.21]	[66.97, 85.68]	[85.48, 90.85]	
Early Fusion Baseline	83.60	81.83	90.95	85.79	76.70	75.41	88.25	78.14	86.49	-
	[83.03, 84.17]	[81.19, 82.48]	[90.66, 91.23]	[85.35, 86.23]	[75.97, 77.43]	[74.30, 76.52]	[87.84, 88.67]	[77.26, 79.02]	[85.69, 87.29]	
Hybrid Fusion Baseline	84.09	82.35	91.37	86.50	77.33	76.18	88.52	78.58	87.00	-
	[83.77, 84.42]	[81.98, 82.72]	[91.17, 91.56]	[86.21, 86.79]	[76.93, 77.73]	[75.46, 76.91]	[88.24, 88.80]	[77.93, 79.22]	[86.44, 87.57]	
<i>UFNet</i> - Early Fusion	86.70	85.83	92.65	86.20	79.92	83.34	88.33	76.88	91.87	-
	[86.24, 87.15]	[85.38, 86.29]	[92.39, 92.91]	[85.55, 86.85]	[79.10, 80.73]	[82.68, 84.01]	[87.71, 88.94]	[75.45, 78.30]	[91.44, 92.30]	
<i>UFNet</i> - Early Fusion (withhold uncertain predictions)	87.47	86.54	92.92	86.43	80.66	83.97	89.12	77.73	92.43	97.36
	[87.05, 87.89]	[86.10, 86.99]	[92.65, 93.18]	[85.78, 87.09]	[79.88, 81.45]	[83.23, 84.70]	[88.55, 89.69]	[76.37, 79.09]	[91.99, 92.86]	[97.05, 97.67]
<i>UFNet</i> - Hybrid Fusion	87.29	86.39	92.81	86.28	80.96	83.78	89.00	78.38	91.99	-
	[86.93, 87.66]	[86.01, 86.77]	[92.60, 93.01]	[85.81, 86.76]	[80.35, 81.58]	[83.24, 84.32]	[88.56, 89.43]	[77.40, 79.36]	[91.67, 92.31]	
<i>UFNet</i> - Hybrid Fusion (withhold uncertain predictions)	88.04	87.13	93.04	86.52	81.82	84.58	89.68	79.28	92.56	97.75
	[87.72, 88.36]	[86.81, 87.45]	[92.84, 93.24]	[86.04, 87.00]	[81.28, 82.35]	[84.09, 85.07]	[89.26, 90.10]	[78.37, 80.18]	[92.29, 92.82]	[97.45, 98.05]

UFNet performs better than other multi-modal fusion baselines

The proposed uncertainty-calibrated fusion network (*UFNet*) outperforms all the four baseline methods in most metrics (see Table 3). Although the neural late fusion baseline achieves the best AUPRC, the average F_1 score is notably lower compared to other baselines and the *UFNet* choices. The model also has the least stability (therefore, dependent on the random seed) as the confidence interval is large for most metrics. *UFNet* significantly improves the accuracy, balanced accuracy, positive predictive value (PPV), and specificity over the baselines. The other metrics are non-inferior compared to the baselines.

In general, providing task-specific predictions as additional input (i.e., hybrid fusion) slightly improves model performance. Withholding uncertain prediction also helps boost performance. With dropping the uncertain predictions, the best *UFNet* (Hybrid fusion) model achieves $88.04 \pm 0.32\%$ accuracy, $87.13 \pm 0.32\%$ balanced accuracy, $93.04 \pm 0.20\%$ AUROC (see Figure 2a), and $81.82 \pm 0.53\%$ F_1 score, better than any other model choices. The model also achieves the best PPV ($84.58 \pm 0.49\%$), NPV ($89.68 \pm 0.42\%$), sensitivity ($79.28 \pm 0.90\%$), and specificity ($92.56 \pm 0.26\%$). However, instead of predicting on all data, the model can now cover $97.75 \pm 0.30\%$ data where it is certain enough to predict.

The expected calibration error (ECE) of the model is $5.4 \pm 0.5\%$ and the Brier score is 0.097 ± 0.002 , indicating that the model predicted probability is aligned with true disease probability (see Figure 2b).

Performance based on demographic attributes

We did not observe any significant bias in model performance (evaluated on the test set consisting of 162 individuals) based on sex and race. The average error (i.e., miss-classification) rate across the female participants ($n = 85$) was $14.1 \pm 7.4\%$, while the rate was $6.5 \pm 5.5\%$ for the male participants ($n = 77$). This difference in performance is notable, but not statistically significant ($p\text{-value} = 0.11$). The error rate was $7.63 \pm 4.79\%$ for white participants ($n = 118$) and $5.56 \pm 11.39\%$ for Non-white participants ($n = 18$). Based on Fisher's exact test, this difference was also non-significant (Fisher's odd ratio = 0.71, $p\text{-value} = 1.0$). However, the error rate of the proposed PD detection model notably varied based on age subgroups. The model performed relatively well for individuals aged between 50 and 80, while the error rate was higher among individuals aged between 30 and 50, or over 80. The lower performance may be due lacking data from individuals of these age groups. For instance, our dataset mostly consists of 50-80 year old individuals (77.1% of the entire dataset).

DISCUSSION

Video analysis offers an accessible, cost-effective, and convenient means of screening for PD, that would be particularly beneficial for individuals in remote areas or low-income countries where access to neurological care is limited. Building upon prior work demonstrating the feasibility of classifying PD symptoms from single video tasks [2, 11, 20], this study explored using a combination of three tasks for a more holistic and generalizable approach, reflecting the multifaceted nature of PD symptoms. Utilizing webcam recordings of individuals (with and without PD) performing finger tapping, speech, and smile tasks, we developed machine learning models to classify PD cases with high accuracy, sensitivity, and specificity. In addition, our model provides uncertainty estimates, withholding predictions in low-confidence scenarios.

We carefully weighed the feasibility and safety considerations when selecting the three proposed tasks for remote completion. The selected tasks enable the assessment of bradykinesia, hypomimia, and speech impairment. Notably, all can be safely performed at home without requiring assistance. While gait analysis, like the 10-meter walk test, is a common component for the evaluation of PD [13, 14], it presents logistical challenges for home recordings and potential fall risks for participants. In contrast, the finger-tapping task is a safer alternative for motor assessment. Neurologists assess facial expressions and speech through natural conversations. However, prompting natural conversations introduces subjectivity and confounding factors like speech length, hindering machine learning model training, especially with limited data. Mimicking a smile, a familiar action similar to posing for a camera, offers a standardized alternative. Similarly, the pangram utterance task reduces the impact of confounding factors on speech analysis. While sustained phonation (holding a vowel sound for as long as possible) is another speech assessment option [24, 25], its analysis becomes complicated due to inconsistencies across various recording devices. All of the selected tasks had reasonable predictive performance in differentiating among individuals with and without PD, demonstrating the effectiveness of task selection.

Models that were trained on all three tasks performed better than models trained on any one single task. Of the single-task specific models, PD classifications from the speech task performed the best, however the proposed hybrid fusion model (*UFNet*) trained on all three tasks was our best performing model overall with the highest AUROC, accuracy, recall, and specificity. Withholding uncertain predictions further boosted the performance of the model, ensuring additional safeguards against potential harms of miss-predictions. The performance of the proposed model was also superior to traditional data-efficient neural models for combining multiple modalities.

However, the proposed work has some limitations. To begin with, our model performs consistently across sex and race subgroups, but accuracy drops for younger (30-49) and older (above 80) age groups. Table 1a shows an

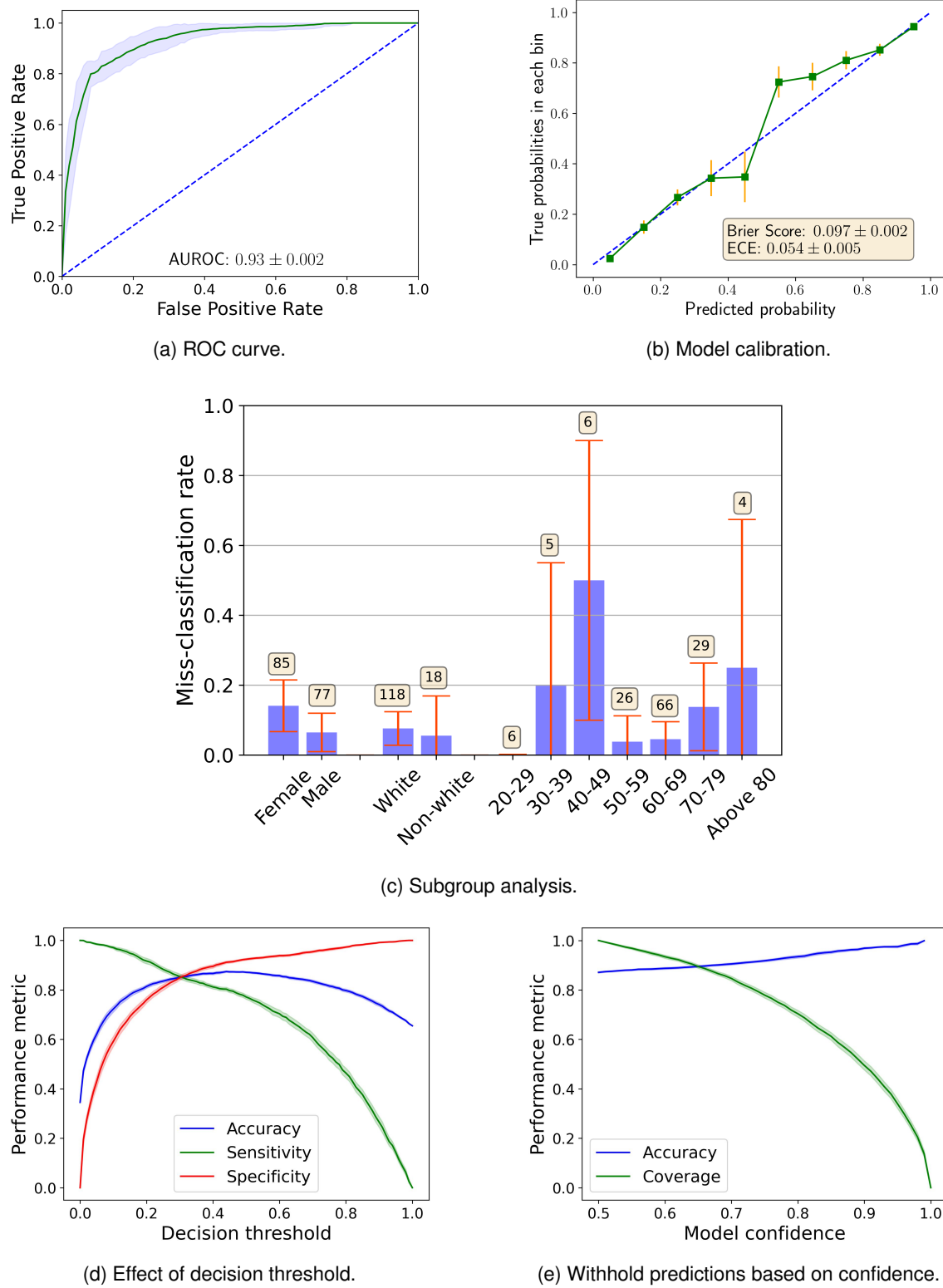


Fig. 2. Visualization of model performance. The shaded regions (a, d, e) or the error bars (b, c) represent 95% confidence intervals.

underrepresentation of these participants in our dataset, with over 75% falling between 50 and 80 years old. This age bias likely explains the model's stronger performance in this middle range. To ensure safe and generalizable use, we recommend applying the tool only to individuals between 50 and 80 years old until a more balanced dataset is available. Future work should prioritize recruiting younger and older participants.

In addition, the thresholds used in the study could be further customized based on individual preference. The decision threshold, which separates PD from non-PD based on the model's predicted probability, directly affects the model's sensitivity and specificity (as shown in Figure 2d). We used the common 0.5 threshold for this study, but individual preferences for risk-benefit trade-offs might necessitate adjustments. For instance, some users might seek clinical evaluation even at lower probabilities (i.e., prefer a model with high sensitivity), while others might wait for a higher likelihood before incurring healthcare costs (i.e., prefer high specificity). During clinical integration, this threshold can be customized based on individual needs and existing healthcare infrastructure. Also, we chose to withhold predictions when the model is uncertain about the PD/non-PD classification. Specifically, if the 95% confidence interval of the prediction contains both positive and negative class, the model refrains from making a prediction. In the absence of MC dropout (or when obtaining multiple rounds of predictions is costly), an alternative would be interpreting the model prediction scores as its confidence. For example, a predicted positive class score of 80% can be treated as a PD prediction with 80% confidence. Based on accuracy-coverage trade-off (and participant preference), a suitable confidence level could be selected (Figure 2e), whereas, a prediction will be withheld if the model confidence is below that level.

Furthermore, as videos are primarily gathered in an unsupervised fashion, issues such as noncompliance with task instructions and various forms of noise are common occurrences. For example, during the finger-tapping task, many participants performed fewer than the required ten taps, often with their task-performing hand obscured from view within the recording frame. Similarly, background noise may distort speech features, while the presence of multiple individuals in the frame could compromise the accuracy of smile feature extraction. Integrating post-hoc quality assessment algorithms into the data collection framework in the future could further enhance data quality. These algorithms could identify the quality issues, and if needed, prompt the user to re-record one or more tasks.

Finally, while we have experimented our model on the largest available video dataset in the literature, validating it across multiple datasets would strengthen our confidence in its effectiveness. Unfortunately, patient videos, being protected health information, are not publicly accessible. Hence, we could not gather multiple datasets of videos or extract similar features.

In conclusion, this study demonstrates the promising efficacy of machine learning models in distinguishing individuals with PD from those without PD, requiring only a laptop equipped with a webcam, microphone, and internet connection. Given the shared characteristics and nuanced distinctions among movement disorders such as PD, Huntington's disease, ataxia, and Progressive Supranuclear Palsy, these findings hold significant implications. We hope that the promising initial results from this research will pave the way for extending tele-neurology applications to encompass a broader range of movement disorders.

CONTRIBUTORS

The study was conceptualized by MSI, JF, and EH, who also co-wrote the manuscript. MSI took the lead in developing, implementing, and evaluating the machine learning models, while JF specifically proposed the application of Monte Carlo dropout and refined the model architecture. TA, SL, and AA all contributed to running the experiments. Data collection was coordinated by CS and KJ for the PD wellness center cohort, and by MP for the clinical study participants. RBS and ERD were the clinical co-PIs and provided invaluable guidance in grounding the research health integration. EH is the PI for the project. Finally, all authors participated in reviewing and editing the manuscript.

DECLARATION OF INTERESTS

All the authors declare that there are no competing interests.

DATA SHARING

The recorded videos were collected using a web-based tool. The tool is publicly accessible at <https://parktest.net>. The codes for video processing, feature extraction, and model training will be made publicly available upon the acceptance of this paper. We will provide a link to the repository containing the codes. Unfortunately, we are unable to share the raw videos due to the Health Insurance Portability and Accountability Act (HIPAA) compliance. However, we are committed to sharing the dataset of the extracted features upon receiving an email request at rochesterhci@gmail.com. The features will be provided in a structured format that can be easily integrated with existing machine-learning workflows.

ACKNOWLEDGMENTS

The project was supported by the National Science Foundation Award IIS-1750380, National Institute of Neurological Disorders and Stroke of the National Institutes of Health under award number P50NS108676, and Gordon and Betty Moore Foundation. The first author (MSI) is supported by a Google PhD fellowship.

DISCLOSURES

Dr. Dorsey has received honoraria from the American Neurological Association, Kairos Cinema, Texas Neurological Society, and University of Toronto; received compensation for consulting services from Abbvie, Adivo Associates, Bial-Biotech Investments, Inc., Biohaven Pharmaceuticals, Biosensics, Boehringer Ingelheim, California Pacific Medical Center, Caraway Therapeutics, Cerevance, Deallus, Genentech/Roche, Grand Rounds, HMP Education, Mediflix, MedRhythms, Medscape, Merck, Mitsubishi Tanabe Pharma, NACCME, NeuroDerm, NIH, Novartis, Otsuka, PRIME Education, Sanofi, Seelos Therapeutics, Sutter Home, and WebMD; research support from Averitas Pharma, Biogen, Burroughs Wellcome Fund, Department of Defense, Michael J. Fox Foundation, National Institutes of Health, PhotoPharmics, Roche, and Thomas Golisano Foundation; editorial services for Karger Publications; stock in Included Health and Mediflix and ownership interests in Synapticure and SemCap.

SUPPLEMENTARY NOTE 1. HYPER-PARAMETERS FOR THE TASK-SPECIFIC MODELS

Task-specific models without Monte Carlo dropout

The hyper-parameter search space is outlined in Table 4.

Hyperparameter	Values/range	Distribution
batch size	{256, 512, 1024}	Categorical
learning rate	[0.0005, 1.0]	Uniform
drop correlated features?	{"yes", "no"}	Categorical
correlation threshold	{0.80, 0.85, 0.90, 0.95}	Categorical
use feature scaling?	{"yes", "no"}	Categorical
scaling method	{"StandardScaler", "MinMaxScaler"}	Categorical
use minority oversampling (i.e., SMOTE)?	{"yes", "no"}	Categorical
number of hidden layers	{0, 1}	Categorical
number of epochs	[1, 100]	Uniform Integer
optimizer	{"SGD", "AdamW"}	Categorical
momentum	[0.1, 1.0]	Uniform
use scheduler?	{"yes", "no"}	Categorical
scheduler	{"step", "reduce on plateau"}	Categorical
step size	[1, 30]	Uniform Integer
patience	[1, 20]	Uniform Integer
gamma	[0.5, 0.95]	Uniform
seed	[100, 999]	Uniform

Table 4. Hyper-parameter search space for the task-specific models (without MC dropout).

The selected hyper-parameters for the task-specific models are mentioned below:

Finger-tapping task (both hands): batch size = 256, learning rate = 0.6246956232061768, drop correlated features? = no, use feature scaling? = yes, scaling method = StandardScaler, use minority oversampling? = no, number of hidden layers = 0, number of epochs = 82, optimizer = SGD, momentum = 0.8046223742478498, use scheduler? = no, seed = 276

Finger-tapping task (left hand): batch size = 512, learning rate = 0.807750048295928, drop correlated features? = yes, correlation threshold = 0.95, use feature scaling? = yes, scaling method = StandardScaler, use minority oversampling? = no, number of hidden layers = 0, number of epochs = 50, optimizer = SGD, momentum = 0.6614402107331798, use scheduler? = no, seed = 556

Finger-tapping task (right hand): batch size = 512, learning rate = 0.5437653223933676, drop correlated features? = no, use feature scaling? = yes, scaling method = StandardScaler, use minority oversampling? = no, number of hidden layers = 1, number of epochs = 74, optimizer = SGD, momentum = 0.709095892070382, use scheduler? = no, seed = 751

Smile: batch size = 1024, learning rate = 0.8365099039036598, drop correlated features? = no, use feature scaling? = yes, scaling method = StandardScaler, use minority oversampling? = yes, number of hidden layers = 0, number of epochs = 74, optimizer = SGD, momentum = 0.615229008837764, use scheduler? = yes, scheduler = reduce on plateau, patience = 4, seed = 488

Speech: batch size = 256, learning rate = 0.06573643554880117, drop correlated features? = no, use feature scaling? = yes, scaling method = StandardScaler, use minority oversampling? = no, number of hidden layers = 1, number of epochs = 27, optimizer = SGD, momentum = 0.5231696483982686, use scheduler? = no, seed = 287

Task-specific models with Monte Carlo dropout

The hyper-parameter search space is outlined in Table 5.

Hyperparameter	Values/range	Distribution
batch size	{256, 512, 1024}	Categorical
learning rate	[0.0005, 1.0]	Uniform
drop correlated features?	{"yes", "no"}	Categorical
correlation threshold	{0.80, 0.85, 0.90, 0.95}	Categorical
use feature scaling?	{"yes", "no"}	Categorical
scaling method	{"StandardScaler", "MinMaxScaler"}	Categorical
use minority oversampling (i.e., SMOTE)?	{"yes", "no"}	Categorical
number of hidden layers	{0, 1}	Categorical
dropout probability	[0.01, 0.30]	Uniform
number MC dropout rounds	{100, 300, 500, 1000, 3000, 5000, 10000}	Categorical
number of epochs	[1, 100]	Uniform Integer
optimizer	{"SGD", "AdamW"}	Categorical
momentum	[0.1, 1.0]	Uniform
use scheduler?	{"yes", "no"}	Categorical
scheduler	{"step", "reduce on plateau"}	Categorical
step size	[1, 30]	Uniform Integer
patience	[1, 20]	Uniform Integer
gamma	[0.5, 0.95]	Uniform

Table 5. Hyper-parameter search space for the task-specific models (with MC dropout).

The selected hyper-parameters for the task-specific models are mentioned below:

Finger-tapping task: batch size = 256, learning rate = 0.3081959128766984, drop correlated features? = no, use feature scaling? = yes, scaling method = StandardScaler, use minority oversampling? = no, number of hidden layers = 0, dropout probability = 0.24180259124462203, number of MC dropout rounds = 1000, number of epochs = 87, optimizer = SGD, momentum = 0.9206317439937552, use scheduler? = yes, scheduler = reduce on plateau, patience = 13, seed = 790

Smile task: batch size = 256, learning rate = 0.03265227174722892, drop correlated features? = no, use feature scaling? = yes, scaling method = StandardScaler, use minority oversampling? = yes, number of hidden layers = 0, dropout probability = 0.10661756438565197, number of MC dropout rounds = 1000, number of epochs = 64, optimizer = SGD, momentum = 0.5450637936769563, use scheduler? = no, seed = 462

Speech task: batch size = 1024, learning rate = 0.364654919080181, drop correlated features? = yes, correlation threshold = 0.95, use feature scaling? = no, use minority oversampling? = no, number of hidden layers = 0, dropout probability = 0.23420212038821583, number of MC dropout rounds = 10000, number of epochs = 74, optimizer = AdamW, use scheduler? = no, seed = 303

SUPPLEMENTARY NOTE 2. HYPER-PARAMETERS FOR THE UFNFT MODELS

The hyper-parameter search space is outlined in Table 6.

Hyperparameter	Values/range	Distribution
batch size	{256, 512, 1024}	Categorical
learning rate	$[5e^{-5}, 1.0]$	Uniform
use minority oversampling?	{"yes", "no"}	Categorical
oversampling method	{"SMOTE", "SVMSMOTE", "ADASYN", "BoarderlineSMOTE", "SMOTEN", "RandomOversampler"}	Categorical
number of hidden layers	{1}	Categorical
projection dimension	{128, 256, 512}	Categorical
query (query/key/value) dimension	{32, 64, 128, 256}	Categorical
hidden dimension	{4, 8, 16, 32, 64, 128}	Categorical
dropout probability	[0.05, 0.50]	Uniform
η	[0.1, 100]	Uniform
number MC dropout rounds	{30}	Categorical
number of epochs	[1, 300]	Uniform Integer
optimizer	{"SGD", "AdamW", "RMSprop"}	Categorical
momentum	[0.1, 1.0]	Uniform
use scheduler?	{"yes", "no"}	Categorical
scheduler	{"step", "reduce on plateau"}	Categorical
step size	[1, 30]	Uniform Integer
patience	[1, 20]	Uniform Integer
gamma	[0.5, 0.95]	Uniform

Table 6. Hyper-parameter search space for the UFNet models.

The selected hyper-parameters are mentioned below:

Finger-tapping + Smile + Speech: batch size = 1024, learning rate = 0.04696835878517764, use minority oversampling? = no, number of hidden layers = 1, projection dimension = 512, query dimension = 32, hidden dimension = 32, dropout probability = 0.4886014578622704, η = 66.22989673611967, number of MC dropout rounds = 30, number of epochs = 233, optimizer = SGD, momentum = 0.259212523900994, use scheduler? = yes, scheduler = step, step size = 13, gamma = 0.8811368627440624, seed=892

Finger-tapping + Smile: batch size = 256, learning rate = 0.06754950185131235, use minority oversampling? = no, number of hidden layers = 1, projection dimension = 512, query dimension = 64, hidden dimension = 64, dropout probability = 0.4453733432524283, η = 12.554916213821272, number of MC dropout rounds = 30, number of epochs = 18, optimizer = SGD, momentum = 0.9822830376765904, use scheduler? = yes, scheduler = reduce on plateau, patience = 10, seed=919

Finger-tapping + Speech: batch size = 512, learning rate = 0.04035092571261426, use minority oversampling? = no, number of hidden layers = 1, projection dimension = 256, query dimension = 256, hidden dimension = 16, dropout probability = 0.49813214914563847, η = 79.95872101951133, number of MC dropout rounds = 30, number of epochs = 164, optimizer = SGD, momentum = 0.24020164138826405, use scheduler? = yes, scheduler = reduce on plateau, patience = 12, seed=953

Smile + Speech: batch size = 512, learning rate = 0.16688970966723005, use minority oversampling? = no, number of hidden layers = 1, projection dimension = 128, query dimension = 64, hidden dimension = 4, dropout probability = 0.3763157755397192, η = 51.88439832518041, number of MC dropout rounds = 30, number of epochs = 132, optimizer = SGD, momentum = 0.22419387711544064, use scheduler? = yes, scheduler = reduce on plateau, patience = 13, seed=845

SUPPLEMENTARY NOTE 3 – RELATED WORKS

Table 7. Summary of background studies on video and audio analysis for Parkinson's Disease detection and progression tracking.

Study	Data	Data collection setup	Dataset size	Extracted features	Model	Performance
Adnan and Islam et al. (2023) [2]	Videos of mimicked smile expressions	Home, PD care facility, and clinic	1059 participants (256 with PD)	Facial action unit and landmark features	Hist-Gradient-Boost models	90.1% AUROC and 88.0% accuracy based on cross-validation; 82.0% AUROC and 80.0% accuracy on external test data. F_1 score was not reported.
Novotny et al. (2014) [18]	Videos of freely-speech monologue capturing natural facial muscle movements	A room with controlled lighting and a fixed-place camera	166 participants (91 with PD)	Motion across facial regions (e.g., forehead, nose root, eyebrows, eyes, cheeks, mouth, and jaw)	Binary logistic regression classifier	Leave-one-patient-out cross validation: 87.0% AUROC and 78.3% accuracy
Adnan and Abdelkader et al. (2024) [1]	Pangram utterance ("quick brown fox")	Home, PD care facility, and clinic	1306 participants (392 with PD)	Deep embedding from semi-supervised speech models	Neural network	88.9% AUROC, 85.7% accuracy, and 71.1% F_1 score.
Rahman et al. (2021) [20]	Pangram utterance ("quick brown fox")	Home and clinic	726 participants (262 with PD)	Acoustic features such as MFCC, jitter, and shimmer variants	XGBoost	75.0% AUROC and 74.1% accuracy
Almeida et al. (2019) [3]	Two speech tasks: sustained phonation (of vowel a), and pronunciation of a short sentence in Lithuanian	Fixed microphones	120 participants (60 with PD)	Acoustic features such as MFCC, jitter, and shimmer variants	SVM, k-nearest neighbor, Random forest, Naive Bayes	94.55% accuracy and 0.87 AUC using an acoustic cardioid microphone; 92.94% accuracy and 0.92 AUROC using a smartphone
Pah et al. (2022) [19]	sustained phonation of vowels (PC-GITA and Viswanathan datasets)	A noise-restricted environment and a fixed, commercial microphone	PC-GITA dataset: 100 individuals (50 with PD) Viswanathan dataset: 46 individuals (24 with PD)	Voice intensity parameters, periodicity and stability of glottal vibration, and vocal tract characteristics	Support vector machine	Leave-one-out cross-validation: 84.3% accuracy, 84.0% sensitivity, and 84.0% specificity in PC-GITA dataset; 96% accuracy in Viswanathan dataset
Islam et al. (2023) [11]	Finger-tapping videos	Home and clinic	250 total participants (172 PD)	Finger-tapping features including speed, amplitude, hesitations, slowing, and rhythm	LightGBM regressor to predict the MDS-UPDRS finger-tapping severity score	Leave-one-patient-out cross-validation: 0.66 Pearson's Correlation Coefficient and 0.58 mean absolute error compared to clinical ratings
Yang et al. (2024) [28]	Finger-tapping videos	Fixed room and camera. Videos recorded using side-view capture to ensure detailed observation of the movements	186 participants (103 with PD, 24 with atypical parkinsonism, 12 with mild Parkinsonism, and 47 healthy controls)	3D hand key-points	Convolutional neural network (CNN) + data augmentation	81.5% and 88.0% acceptable accuracy in differentiating between moderate/severe and none/slight bradykinesia.

REFERENCES

- [1] ADNAN, T., ABDELKADER, A., LIU, Z., HOSSAIN, E., PARK, S., ISLAM, M., AND HOQUE, E. A novel fusion architecture for pd detection using semi-supervised speech embeddings. *arXiv preprint arXiv:2405.17206* (2024).
- [2] ADNAN, T., ISLAM, M. S., RAHMAN, W., LEE, S., TITHI, S. D., NOSHIN, K., SARKER, I., RAHMAN, M. S., AND HOQUE, E. Unmasking parkinson's disease with smile: An ai-enabled screening framework. *arXiv preprint arXiv:2308.02588* (2023).
- [3] ALMEIDA, J. S., REBOUÇAS FILHO, P. P., CARNEIRO, T., WEI, W., DAMAŠEVIČIUS, R., MASKELIŪNAS, R., AND DE ALBUQUERQUE, V. H. C. Detecting parkinson's disease with sustained phonation and speech signals using machine learning techniques. *Pattern Recognition Letters* 125 (2019), 55–62.
- [4] ATIGHEHCHIAN, P., BRANCHAUD-CHARRON, F., FREYBERG, J., PARDINAS, R., SCHELL, L., AND PEARSE, G. Baal, a bayesian active learning library. <https://github.com/baal-org/baal/>, 2022.
- [5] BANDINI, A., ORLANDI, S., ESCALANTE, H. J., GIOVANNELLI, F., CINCOTTA, M., REYES-GARCIA, C. A., VANNI, P., ZACCARA, G., AND MANFREDI, C. Analysis of facial expressions in parkinson's disease through video-based automatic methods. *Journal of neuroscience methods* 281 (2017), 7–20.
- [6] CHEN, S., WANG, C., CHEN, Z., WU, Y., LIU, S., CHEN, Z., LI, J., KANDA, N., YOSHIOKA, T., XIAO, X., ET AL. Wavlm: Large-scale self-supervised pre-training for full stack speech processing. *IEEE Journal of Selected Topics in Signal Processing* 16, 6 (2022), 1505–1518.
- [7] DORSEY, E., SHERER, T., OKUN, M. S., AND BLOEM, B. R. The emerging evidence of the parkinson pandemic. *Journal of Parkinson's disease* 8, s1 (2018), S3–S8.
- [8] DORSEY, E. R., ELBAZ, A., NICHOLS, E., ABBASI, N., ABD-ALLAH, F., ABDELALIM, A., ADSUAR, J. C., ANSHA, M. G., BRAYNE, C., CHOI, J.-Y. J., ET AL. Global, regional, and national burden of parkinson's disease, 1990–2016: a systematic analysis for the global burden of disease study 2016. *The Lancet Neurology* 17, 11 (2018), 939–953.
- [9] GOETZ, C. G., TILLEY, B. C., SHAFTMAN, S. R., STEBBINS, G. T., FAHN, S., MARTINEZ-MARTIN, P., POEWE, W., SAMPAIO, C., STERN, M. B., DODEL, R., ET AL. Movement disorder society-sponsored revision of the unified parkinson's disease rating scale (mds-updrs): scale presentation and clinimetric testing results. *Movement disorders: official journal of the Movement Disorder Society* 23, 15 (2008), 2129–2170.
- [10] HUGHES, A. J., DANIEL, S. E., KILFORD, L., AND LEES, A. J. Accuracy of clinical diagnosis of idiopathic parkinson's disease: a clinico-pathological study of 100 cases. *Journal of neurology, neurosurgery & psychiatry* 55, 3 (1992), 181–184.
- [11] ISLAM, M. S., RAHMAN, W., ABDELKADER, A., LEE, S., YANG, P. T., PURKS, J. L., ADAMS, J. L., SCHNEIDER, R. B., DORSEY, E. R., AND HOQUE, E. Using ai to measure parkinson's disease severity at home. *npj Digital Medicine* 6, 1 (2023), 156.
- [12] JIN, B., QU, Y., ZHANG, L., AND GAO, Z. Diagnosing parkinson disease through facial expression recognition: video analysis. *Journal of medical Internet research* 22, 7 (2020), e18697.
- [13] LI, A., AND LI, C. Detecting parkinson's disease through gait measures using machine learning. *Diagnostics* 12, 10 (2022), 2404.
- [14] LIU, Y., ZHANG, G., TAROLLI, C. G., HRISTOV, R., JENSEN-ROBERTS, S., WADDELL, E. M., MYERS, T. L., PAWLIK, M. E., SOTO, J. M., WILSON, R. M., ET AL. Monitoring gait at home with radio waves in parkinson's disease: A marker of severity, progression, and medication response. *Science Translational Medicine* 14, 663 (2022), eadc9669.
- [15] LIU, Z., NING, J., CAO, Y., WEI, Y., ZHANG, Z., LIN, S., AND HU, H. Video swin transformer. In *Proceedings of the IEEE/CVF conference on computer vision and pattern recognition* (2022), pp. 3202–3211.
- [16] MOREAU, C., ROUAUD, T., GRABLI, D., BENATRU, I., REMY, P., MARQUES, A.-R., DRAPIER, S., MARIANI, L.-L., ROZE, E., DEVOS, D., ET AL. Overview on wearable sensors for the management of parkinson's disease. *npj Parkinson's Disease* 9, 1 (2023), 153.
- [17] NIXON, J., DUSENBERRY, M. W., ZHANG, L., JERFEL, G., AND TRAN, D. Measuring calibration in deep learning. In *CVPR workshops* (2019), vol. 2.
- [18] NOVOTNY, M., RUSZ, J., CMEJLA, R., AND RUZICKA, E. Automatic evaluation of articulatory disorders in parkinson's disease. *IEEE/ACM Transactions on Audio, Speech, and Language Processing* 22, 9 (2014), 1366–1378.
- [19] PAH, N. D., MOTIN, M. A., AND KUMAR, D. K. Phonemes based detection of parkinson's disease for telehealth applications. *Scientific Reports* 12, 1 (2022), 9687.
- [20] RAHMAN, W., LEE, S., ISLAM, M. S., ANTONY, V. N., RATNU, H., ALI, M. R., MAMUN, A. A., WAGNER, E., JENSEN-ROBERTS, S., WADDELL, E., ET AL. Detecting parkinson disease using a web-based speech task: Observational study. *Journal of medical Internet research* 23, 10 (2021), e26305.
- [21] RUFIBACH, K. Use of brier score to assess binary predictions. *Journal of clinical epidemiology* 63, 8 (2010), 938–939.
- [22] SIDEROWF, A., CONCHA-MARAMBIO, L., LAFONTANT, D.-E., FARRIS, C. M., MA, Y., URENIA, P. A., NGUYEN, H., ALCALAY, R. N., CHAHINE, L. M., FOROUD, T., ET AL. Assessment of heterogeneity among participants in the parkinson's progression markers initiative cohort using α -synuclein seed amplification: a cross-sectional study. *The Lancet Neurology* 22, 5 (2023), 407–417.
- [23] TONG, Z., SONG, Y., WANG, J., AND WANG, L. Videomae: Masked autoencoders are data-efficient learners for self-supervised video pre-training. *Advances in neural information processing systems* 35 (2022), 10078–10093.
- [24] TSANAS, A., LITTLE, M., MCSHARRY, P., AND RAMIG, L. Accurate telemonitoring of parkinson's disease progression by non-invasive speech tests. *Nature Precedings* (2009), 1–1.
- [25] VAICIUKYNAS, E., VERIKAS, A., GELZINIS, A., AND BACAUŠKIENĖ, M. Detecting parkinson's disease from sustained phonation and speech signals. *PloS one* 12, 10 (2017), e0185613.
- [26] VASWANI, A., SHAZEEB, N., PARMAR, N., USZKOREIT, J., JONES, L., GOMEZ, A. N., KAISER, Ł., AND POLOSUKHIN, I. Attention is all you need. *Advances in neural information processing systems* 30 (2017).
- [27] YANG, Y., YUAN, Y., ZHANG, G., WANG, H., CHEN, Y.-C., LIU, Y., TAROLLI, C. G., CREPEAU, D., BUKARTYK, J., JUNNA, M. R., ET AL. Artificial intelligence-enabled detection and assessment of parkinson's disease using nocturnal breathing signals. *Nature medicine* 28, 10 (2022), 2207–2215.
- [28] YANG, Y.-Y., HO, M.-Y., TAI, C.-H., WU, R.-M., KUO, M.-C., AND TSENG, Y. J. Fasteval parkinsonism: an instant deep learning–assisted video-based online system for parkinsonian motor symptom evaluation. *NPJ Digital Medicine* 7, 1 (2024), 1–13.